A Robust Method for Blood Vessel Extraction in Endoscopic Images with SVM-based Scene Classification

Mayank Golhar[1], Yuji Iwahori[2], M. K. Bhuyan[1], Kenji Funahashi[3] and Kunio Kasugai[4]
[1]*Indian Institute of Technology Guwahati, 781039, Guwahati, India*
[2]*Chubu University, 487-8501, Kasugai, Japan*
[3]*Nagoya Institute of Technology, 465-8555, Nagoya, Japan*
[4]*Aichi Medical University, Nagakute, 480-1195, Japan*
mayankgolhar@gmail.com, iwahori@cs.chubu.ac.jp, mkb@iitg.ernet.in, kenji@nitech.ac.jp, kuku3487@aichi-med-u.ac.jp

Keywords: Endoscopy, Scene Classification, SVM, Blood Vessel, Frangi Vesselness.

Abstract: This paper proposes a model for blood vessel detection in endoscopic images. A novel SVM-based scene classification of endoscopic images is used. This SVM-based model classifies images into four classes on the basis of dye content and blood vessel presence in the scene, using various colour, edge and texture based features. After classification, a vessel extraction method is proposed which is based on the Frangi vesselness approach. In original Frangi Vesselness results, it is observed that many non-blood vessel edges are inaccurately detected as blood vessels. So, two additions are proposed, background subtraction and a novel dissimilarity-detecting filtering procedure, which are able to discriminate between blood vessel and non-blood vessel edges by exploiting the symmetric nature property of blood vessels. It was found that the proposed approach gave better accuracy of blood vessel extraction when compared with the vanilla Frangi Vesselness approach and BCOSFIRE filter, another state-of-art vessel delineation approach.

1 INTRODUCTION

Detection and analysis of blood vessels plays a major role in medical diagnosis in large number of areas like retinopathy, endoscopy etc. The detection and analysis of retinal blood vessels may lead to early diagnosis and prevention of diseases, such as diabetic retinopathy, a leading cause of blindness. Similarly, in case of blood vessels lining the colon wall, changes in the shape and structure of blood vessels are symptoms of various diseases. In inflammatory bowel diseases like Crohn's disease and Ulcerative Colitis, there is an increase in size of vessels. Whereas, a decrease in the size of vessels causes reduced blood supply, leading to Ischemic bowel disease like Ischemic Enterocolitis (Kumar et al., 2014).

While a plethora of blood vessel extraction algorithms are available for retinal images (Fraz et al., 2012), such is not the case with endoscopic images. There are some generic segmentation methods which could be used for endoscopic blood vessel detection, but they are not very accurate due to special conditions encountered in endoscopic images like high specular reflection, non-blood vessel patterns, deformable colon walls etc. Thus, this paper proposes a novel algorithm for blood vessel extraction specific for endoscopic images.

Initially, classification of images into four classes based on whether they contain ink, and whether they contain blood vessels is done using SVM. To the best of our knowledge, this is the first instance of such type of classification been done for endoscopic images. Classification of tumor in endoscope images has been attempted using pit pattern features (Hafner et al., 2007). But this is applicable only for magnified endoscopic images focused on tumor, whereas the method proposed, performs classification using higher level features encompassing the complete image information. Section 2.1 discusses the proposed classification process in detail.

In (Lin et al., 2015), colon wall's blood vessels' branching points and branching segments are considered as features. Their approach is based on Frangi vesselness (Frangi et al., 1998) for blood vessel detection. This is followed by Ridgeness-based Circle Test and Ridgeness-based Segment Test for detecting branching points and branching segments respectively. But their algorithm fails to discriminate between blood vessel edges and edges from structures

Golhar, M., Iwahori, Y., Bhuyan, M., Funahashi, K. and Kasugai, K.
A Robust Method for Blood Vessel Extraction in Endoscopic Images with SVM-based Scene Classification.
DOI: 10.5220/0006192601480156
In *Proceedings of the 6th International Conference on Pattern Recognition Applications and Methods (ICPRAM 2017)*, pages 148-156
ISBN: 978-989-758-222-6

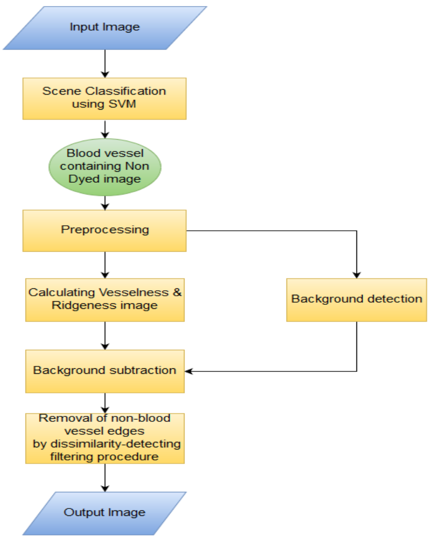

Figure 1: Overview of proposed blood vessel extraction algorithm.

like folds of colon wall, polyp etc. which results in many inaccurate feature points. Thus this paper overcomes these inaccuracies by proposing a collection of techniques to remove the edges obtained from non-blood vessel structures, like dark background subtraction and dissimilarity detecting filtering procedure. The classification and filtering procedure proposed are invariant to orientation, scaling and illumination. Details about these are given in Section 2.3 and 2.4.

2 PROPOSED METHOD

An over view of the approach is shown in the Fig. 1. Initially, scene based classification is done to determine whether the image contains blood vessel information or not. Then, the selected input image is pre-processed to remove specular components. After this step, the blood vessel extraction process begins. The Frangi vesselness and ridgeness image are then calculated. Further, background subtraction is done. In the final step, non-blood vessel edges are identified using dissimilarity-detecting filtering procedure and then removed from Vesselness image to give the final output image. These steps are expounded in following sections.

2.1 Scene-based Classification

2.1.1 Motivation

It is observed that an endoscopic video sequence has an assortment of scenes like frames in which blood vessels are present, frames in which colon is marked with ink with presence or absence of blood vessels, frames with presence or absence of polyps, frames in which the process of tattooing(dyeing) is progress, frames where polyp is been surgically removed, frames where the colon is been washed with medicinal liquid, camera transition from one region of colon to another, scenes containing no clinical information etc. Dyeing, the process of marking colon with ink, is done in colonoscopy for the better visualisation of polyps and marking smaller polyps for future diagnosis.

For the purpose of blood vessel extraction, this multitude of scenes can be broadly divided into four major categories which are as follows:

Class 1 : Blood vessel containing non-dyed images.

Class 2 : No blood vessel containing non-dyed images.

Class 3 : Blood vessel containing dyed images.

Class 4 : No blood vessel containing dyed images.

This classification is necessary as different classes require different blood vessel delineation techniques. This is due to many factors, e.g. in the dyed image classes there is added specularity because of ink liquid, ink pattern texturally similar to vessel pattern leading to detection of false blood vessels etc. However, in this paper we will be focusing on the treatment of non-dyed images containing blood vessels only. Blood vessel extraction from ink images is a topic of future work. Representative images for various classes are shown in Fig 2.

2.1.2 Methodology

With an aim to make classification robust, but not computationally intensive, Support Vector Machine as classifier was used. As SVM is a binary classifier and we have total four classes, One V/s One classification was used. As shown in Section 3.1, it was found that the cubic kernel gave the best classification result.

The major challenge was to define the feature vector which could help differentiate between images of the specified classes. For feature selection, (Mohanty et al., 2013) and (Zhang et al., 2000) were referred. The feature vector was defined on the basis of the following three criteria:

1. **Colour-based Features.** These features are used to differentiate between the non-ink images(more red component) and ink images (more blue component). For every color, the 10 - bin first order histogram values, the mean, variance, skew, energy and entropy are used as features. Thus, the

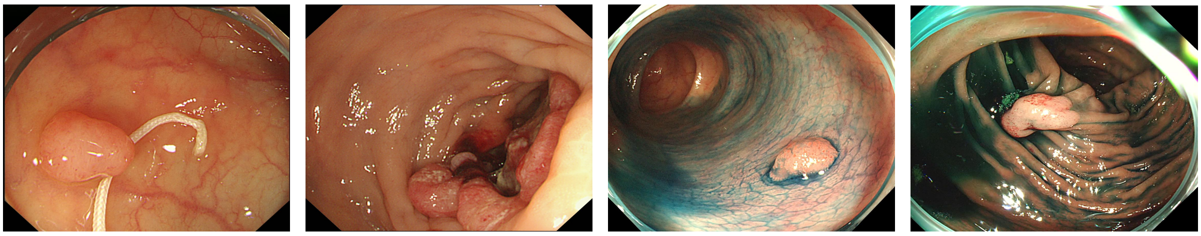

(a) Blood vessel containing non-dyed image - Class 1 (b) No blood vessel containing non-dyed image - Class 2 (c) Blood vessel containing dyed image - Class 3 (d) No blood vessel containing dyed image- Class 4

Figure 2: Representative images of Classes 1 to 4.

total number of colour-based features used were 45.

2. **Edge-based Features.** The Canny edge operator is used on every channel for getting the gradient magnitude and direction. For every color, 10 - bin histogram values, the mean, variance, skew, energy and entropy derived from gradient magnitude are used as features. A histogram of directional angles with central bin values $\{-90°, -45°, 0°, 45°, 90°\}$ is constructed. The histogram bin counts, the mean, variance, skew, energy and entropy obtained from directional angle values are also used as features. The total number of edge-based features used were 75.
3. **Texture-based Features.** To differentiate between the blood vessel and non-blood vessel containing classes, the following features are proposed. Image is first converted to grayscale and then :
   (a) The Fast Fourier Transform (FFT) transform of the image is calculated. The mean, variance, skew, energy, entropy of the FFT and grayscale images are used as features. Also the range of each column of grayscale image is used as feature.
   (b) A gabor filter bank is created, with filters having different wavelengths and orientations. The orientations of gabor filter used are $\{0°, 45°, 90°, 135°\}$ and wavelengths increasing exponential, in range $[2\sqrt{2}$, Hypotenuse of image]. For each filtered image, the 10 - bin histogram values, the mean, variance, skew, energy and entropy are used as features. The total number of texture-based features were 210.

2.2 Blood Vessel Extraction

One of the major challenges while working with endoscopic images is the abundant specular reflection. For removing specular reflection the method proposed by (Ikeda et al., 2016) was used. It is to be noted that the regions identified as specular reflections were treated as no information regions. The proposed method is based on approach described in the paper (Lin et al., 2015). The Frangi vesselness image, which identifies the vessel edges, is obtained using the algorithm suggested in (Frangi et al., 1998). The ridgeness image is a form of skeletonised version of the vesselness image, whose approach is described in (Lin et al., 2015). In the results of these approaches, many non-blood vessel edges were inaccurately identified as blood vessels. For the completeness of paper, their approach is briefly summarized as follows:

1. Pre-Processing
   (a) Extract only green channel of image as it gives best contrast between vessels and background.
   (b) Convert to scale space model.
   (c) Calculate Hessian matrix for each point.
   (d) Calculate the eigenvalue and eigenvector for each point from Hessian matrix. The eigenvalues obtained are say λ_1 and λ_2. The points having λ_1 - Medium value and λ_2 - High value are considered as a candidates of blood vessels.
2. Blood vessel enhancement
   (a) Parameter ridgeness is defined as

$$\begin{aligned} &Ridgeness(x,y,\sigma) \\ &\quad = Vesselness(x,y,\sigma).abs\{ \\ &\qquad sign(\nabla I(x+\varepsilon u_2, y+\varepsilon v_2, \sigma)) \\ &\qquad\quad - sign(\nabla I(x-\varepsilon u_2, y-\varepsilon v_2, \sigma))\}/2, \end{aligned} \tag{1}$$

$$\begin{aligned} Vesselness(\sigma) = \\ &exp(\frac{\lambda_1^2/\lambda_2^2}{2\beta^2})(1 \\ &\quad - exp(\frac{-(\lambda_1^2+\lambda_2^2)}{2c^2})) \end{aligned} \tag{2}$$

where in the ridgeness formula u_2 and v_2 are the x and y components of the eigenvector pointing in the direction perpendicular to that of blood vessel. In the vesselness formula, β and *c* are soft thresholds. Ridgeness for all the candidate points are calculated. Thereafter, the pixels which have local maximum are only retained.

(b) The result of this step is that we obtain single pixels width ridges (representative of blood vessel skeleton). Background noise is also removed.

The further approach, which is the novelty of the paper, aims at removing these non-blood vessel edges from the extracted results image.

2.3 Background removal

2.3.1 Source of Error

In images where the endoscope camera is perpendicular to the walls of colon, the result of blood vessel extraction is acceptable. But, when the image is captured where the endoscope camera is parallel to the colon wall, there is dark background in the image, where false noisy edges are detected as blood vessels, as shown in Fig. 3. To remove this error, an attempt is made to segment dark background region from the foreground.

2.3.2 Methodology

Several approaches were tried to segment the background from foreground namely, Otsu's single level thresholding, k-means clustering and Otsu's multi level thresholding, each of which were tested on the three colour channels. As the results show, the *Otsu's multi-level thresholding using two thresholds using Red channel* is the best, among all investigated methods, for dark background segmentation in endoscopic images. As we are thresholding using two thresholds, we get three clusters among which, the region with the lowest intensity is considered as the dark background region whereas the other two are considered as foreground.

In images captured by camera with orientation parallel to the wall of colon, it was observed that the image can be divided into three different regions based on illumination. The region close to the camera was brightly illuminated, moderate illumination was found in the mid range region and far away region was poorly illuminated. Hence, the results were found to be better when partitioning was done into three clusters. The close by and mid range regions were found to contain useful clinical information and were hence retained, whereas the faraway region, due to lack of illumination did not contain much useful interpretable information and hence was discarded.

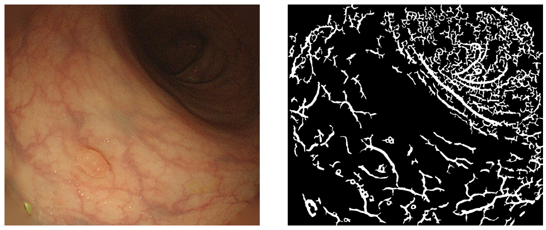

(a) Original image (b) Vessel image

Figure 3: Noisy edges in dark background region identified as blood vessels.

2.4 Removing Non-blood Vessel Edges

2.4.1 Source of Error

In the vesselness image, it is found that along with blood vessels, many ridges or folds of colon walls, polyp edges and specular reflections are also erroneously identified as blood vessel. This section discusses a method to identify and remove ridges, folds of walls and specular components from the result of extracted edges. Vesselness image which contains ridges, polyp edges and specular components is shown in Fig. 4.

2.4.2 Motivation

In endoscopic image, the edges obtained from blood vessel and those from other components like ridges, specular components and polyp edges are fundamentally different, if the intensities of the neighborhood regions of these edges are considered. The differences are as follows:

- **Blood Vessel.** If a window is drawn around the blood vessel with center line of blood vessel dividing the window into two halves as shown in Fig. 5a, it is generally observed that the intensities of both halves of window are similar.

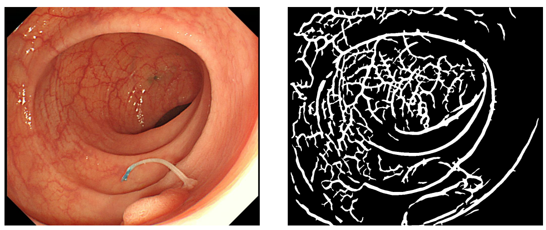

(a) Original image (b) Extracted edges

Figure 4: The ridges of inner walls, polyp and medical suture have been erroneously extracted as blood vessels in vesselness image.

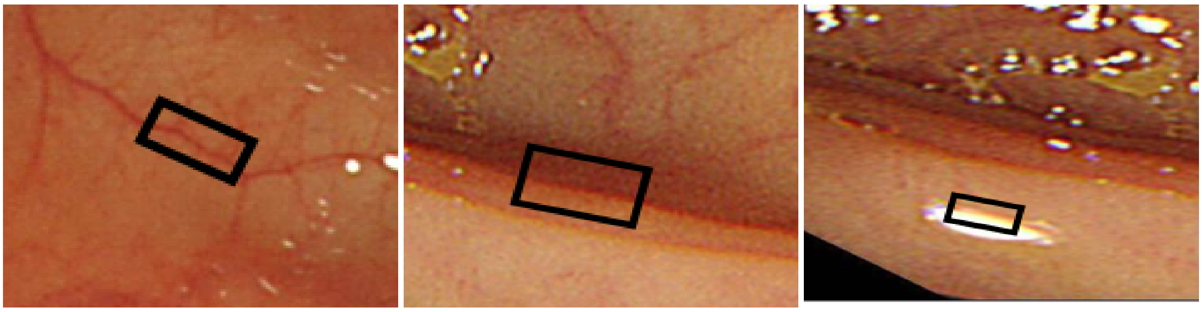

(a) Window around blood vessel (b) Window around ridge (c) Window around specular component

Figure 5: Windows around various structures, showing the differences in intensity in the two halves of window.

- **Ridges, Polyp Edges and Specular Components.** If a similar window is drawn is around the edge of a ridge or polyp or specular component i.e. a window placed such that the center line of the window is on the edge of the ridge, thereby dividing the window into two halves, it is generally observed that intensity-wise these two halves are very dissimilar. Generally, one half is darker and other half is brighter as shown in Fig. 5b and 5c. Also, it is observed that the *vesselness* value of ridges and specular reflection is higher than that of most of the blood vessels.

2.4.3 Overview of the Approach

Based on the above motivation, the intensity difference of the two halves of the window is exploited to identify whether the extracted edge is a blood vessel or not. So, a custom intensity-based dissymmetry detecting filter is proposed. The proposed approach is as follows:

1. An initial thresholding on the basis of vesselness value is done to identify the strong non-blood vessel edges. This generally discards most of the blood vessels, but not all. After thresholding, the edges which remain are generally from ridges, specular components, polyps and some blood vessels.

2. The edges obtained above are then processed to find their center lines. The center lines of the edges can be obtained by *ridgeness* values.

3. After obtaining the center lines of the edges, the custom intensity-based dissymmetry detection filtering is done. The custom filter is a rotating filter, oriented in the direction of blood vessel. The direction of blood vessel is given by the minor eigenvector of the Hessian matrix at the point of filtering. In other words, the rotating filter is oriented such that the center line of the filter coincides with the center line of the edge.

$$f(i,j) = \underset{\theta}{rotate}\frac{1}{25}\begin{pmatrix} -1 & -1 & -1 & -1 & -1 \\ -1 & -1 & -1 & -1 & -1 \\ 0 & 0 & 0 & 0 & 0 \\ 1 & 1 & 1 & 1 & 1 \\ 1 & 1 & 1 & 1 & 1 \end{pmatrix} \tag{3}$$

where θ is the direction of the minor eigenvector, which is along the direction of edge. Another point to be noted is that, due to lack of space the filter size shown is 5×5 pixels but in actual implementation window size of 20×20 pixels was used.

4. The filter is placed along the the center line of the edge. The image used for filtering is the Gaussian smoothened red channel of the original image. The filter effectively finds the sum of intensities values of all pixels lying in each half of the filter, and returns the absolute difference of these two halves sum-of-intensities.

$$g(i,j) = \begin{cases} abs|f(i,j) * x(i,j)| & \text{if } x(i,j) \in \text{Centerline} \\ 0 & \text{otherwise.} \end{cases} \tag{4}$$

where $f(i,j)$ is the custom filter, $x(i,j)$ is the gaussian filtered original image's red channel and $g(i,j)$ is the filtered image.

5. The average of all the filtered values of the center line pixels lying inside an edge, is calculated. This average value, termed as Dissymmetry Index, is then assigned to the respective edge. Mathematically, Dissymmetry index of the k^{th} edge is given by

$$Dissymmetry\,index(k) = \frac{1}{|S_k|}\sum_{g(i,j)\in S_k} g(i,j) \tag{5}$$

where S_k is the set of all pixels of filtered image belonging to the k^{th} edge. $|S_k|$ is the total number of pixels belonging to the k^{th} edge.

6. The edges which have Dissymmetry index above certain threshold, indicating they have contrasting halves, are labeled non-blood vessel edges.

7. The steps 4 to 7 are repeated but, this time the green channel of the original image is used for filtering. This is done, as it is found that some non-blood vessel edges are better detected by the red channel and some by green channel.
8. The results obtained from the red and green channel are then OR'ed and the resulting image generally consists of mostly ridges and specular components and other non-blood vessel edges.
9. The OR'ed image is then subtracted from the extracted edges and thus final result is obtained, which consists mostly of blood vessels.

3 EXPERIMENTS AND RESULTS

3.1 Scene Classification

For the purpose of scene classification, Support vector machine (SVM) model was used. Classification of image into the aforementioned four classes was done. The data set comprised of a total of 513 images with 71, 141, 111 and 190 in Classes 1, 2, 3 and 4 respectively. For ground truth, data set images were manually classified by visual inspection into the classes.

Different kernels were experimented with, to find out which gave the best results. Linear, quadratic, cubic, fine Gaussian, medium Gaussian and coarse Gaussian kernels were used. The results obtained for the kernels are shown in Table 1. The One versus One classification was used as it gave comparatively better results than One versus All classification. For measuring the predictive performance of the statistical model, 10 - fold cross validation was done.

The **One Vs One SVM with cubic kernel** gave the best result. Instead of cubic kernel, quadratic kernel can also be used as the accuracy of the learning algorithm was found to be similar and it takes less computation time. It was observed that if dimensionality

Table 1: Accuracy using different kernels.

Kernel	Accuracy (without PCA)	Accuracy (post PCA)
Linear	81.1%	77 %
Quadratic	84.8 %	78.4%
Cubic	85.4 %	78.4%
Fine Gaussian	39.4 %	38.4%
Medium Gaussian	82.5 %	71.3%
Coarse Gaussian	57.7 %	37%

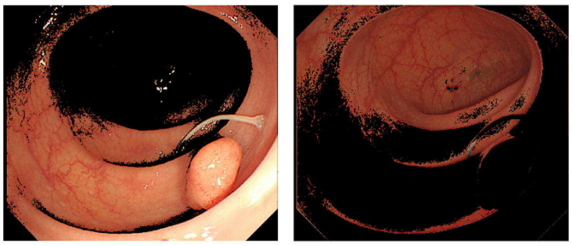

Figure 6: Adaptive single threshold based clustering did not give acceptable result.

reduction is done using Principal component analysis (PCA), the accuracy fell by 5-7% even if the variance retained is 99%. The post PCA results are shown in the Table 1.

3.2 Background Removal

To achieve the goal of background removal, various approaches were tried. A discussion on the methodologies used is given below:

1. **Adaptive Thresholding using Otsu's method : Single threshold** : First a single global threshold is found using Otsu's method, which tires to minimize the intra-class variance. The results of segmentation using a single threshold were not accurate in many images. An example image where it failed is shown in Fig. 6

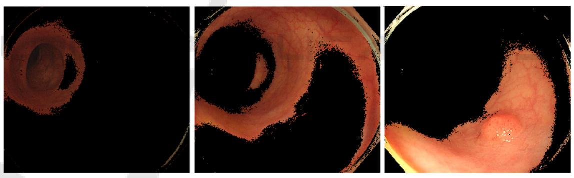

(a) Result of clustering using Red channel values

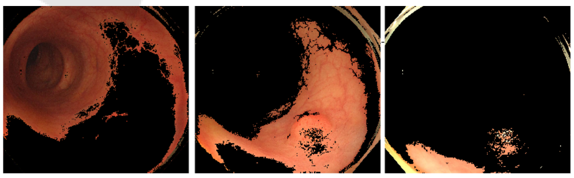

(b) Result of clustering using Green channel values

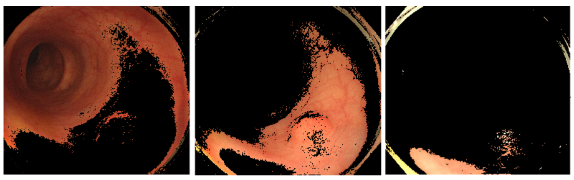

(c) Result of clustering using Blue channel values

Figure 7: Results of K-means clustering using RGB.

2. ***K*-means Clustering.** To segment the dark background from the foreground region, pixel classi-

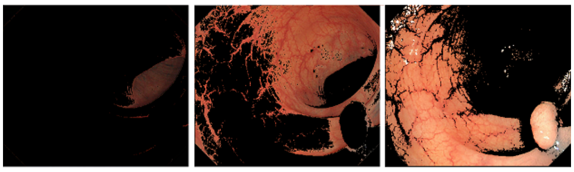

(a) Result of clustering using L* component

(b) Result of clustering using a*b component

Figure 8: Results of *K*-means clustering using Lab.

(a) Result of clustering using Hue component

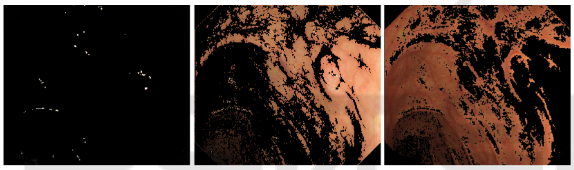

(b) Result of clustering using Saturation component

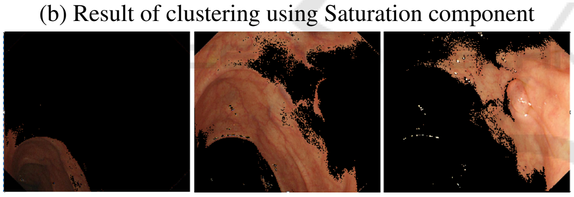

(c) Result of clustering using Value component

Figure 9: Results of *K*-means clustering using HSV.

fication using *k*-means clustering was done. *K*-means clustering was tried using various color space like RGB, CIE-Lab color space and the various channels in these color spaces. Comparison is done to find out which channel of which color space gives the best performance of segmentation. *K*-means clustering was done into three clusters using initial seeds as 0.1, 0.5 and 0.75.

(a) *Comparison between R, G and B color channels* : The following segmentation was observed, when for clustering the Red, Green or Blue channel were used separately. Comparison is shown in Fig 7. It was found that Red color channel gave the best results for segmentation in most cases.

(b) *Comparison between L* and a*b* color channels* : The L*a*b* color space is derived from the CIE XYZ tristimulus values. The L*a*b* space consists of a luminosity 'L*' or brightness layer, chromaticity layer 'a*' indicating where color falls along the red-green axis, and chromaticity layer 'b*' indicating where the color falls along the blue-yellow axis. Comparison between L* and a*b* space is shown in Fig. 8. The best segmentation was done by using L* channel.

(c) *Comparison between H, S and V channels* : A comparison of k-means clustering is done between the H, S and V channels, as shown in Fig.9. It was observed that V channel of the image gave the best results. It's clustering result was similar to the R channel.

(d) *Comparison between R and L* color channels* : Among the RGB and CIE Lab color space the best result was observed using the 'R' and 'L*' channels. So, a comparison is further made be-

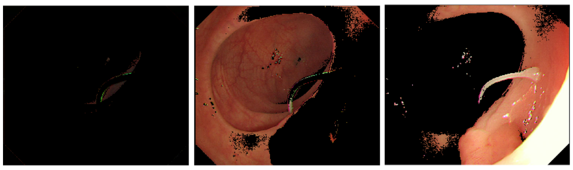

(a) Result of clustering using Red component

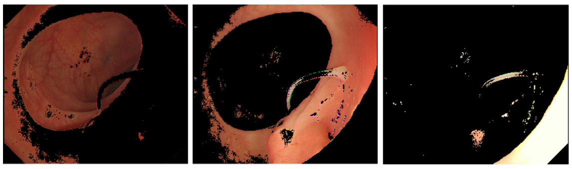

(b) Result of clustering using L* component

Figure 10: *K*-means clustering result comparison of Red and L* components.

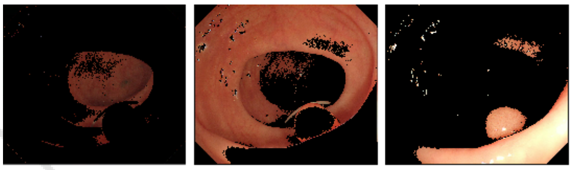

(a) Result of *K*-means clustering

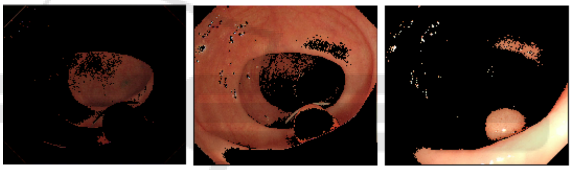

(b) Result of Adaptive thresholding using Otsu's method with 2 thresholds

Figure 11: *K*-means clustering and Adaptive thresholding using Otsu's method with 2 thresholds gave similar results.

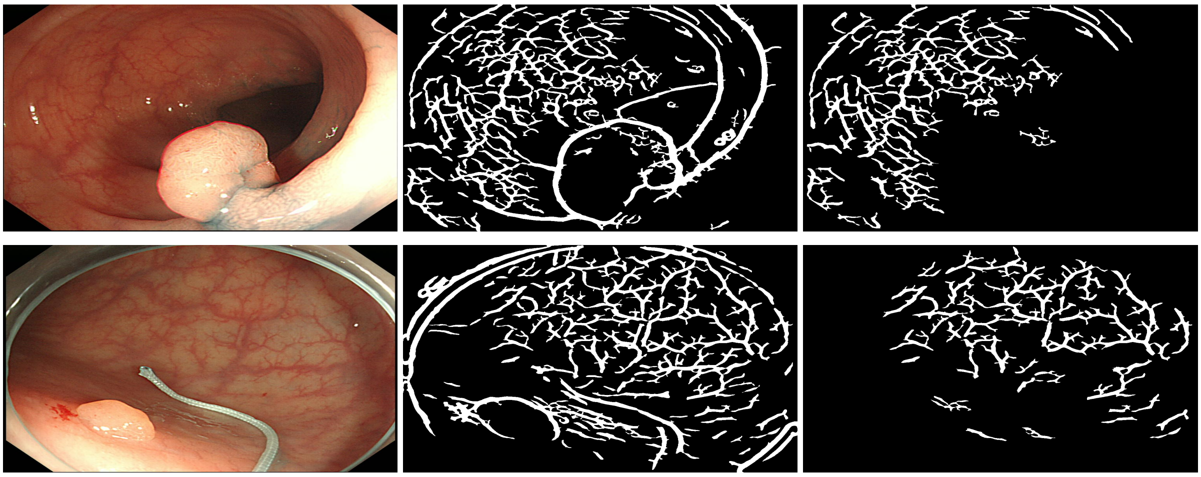

(a) Original Image (b) Vesselness image (c) Final Result

Figure 12: Comparison of input, vesselness and final result.

tween them, as shown in Fig. 10. It was found that using the R channel gave best results.

(e) *Adaptive Thresholding using Otsu's Method using 2 Thresholds* : Multilevel thresholding using the Otsu's method was done using R channel and 3 clusters were obtained . The results obtained by Otsu's multi-level thresholding and k-means clustering were found to be almost the same, as shown in Fig. 11.

As the results of k-means clustering and Otsu's 2 level adaptive thresholding were almost the same, and Otsu's thresholding is faster, it can be concluded that *Otsu's multi-level thresholding using two thresholds on R channel* is the best, among all investigated methods, for dark background segmentation in endoscopic images. Also, it was observed that in images where there are no dark regions the clustering was done automatically into two clusters.

3.3 Removal of Non-blood Vessel Edges

The proposed method removes the non-blood vessel edges by using two approaches. It removes the background region, thereby eliminating the false edges which occur due to image noise. Second, an Dissimilarity Index is used to categorise whether the given edge came from a blood vessel or not.

A dataset of 61 images was used for evaluation. For ground truth, the blood vessel were manually marked in all the images. The values of various thresholds used in evaluation are : Strong edge *vesselness* threshold = 0.9, Red Channel-Dissimilarity Index threshold = 3 and Green Channel-Dissimilarity Index threshold = 3. These values were found to give the best result empirically. The comparison of various algorithms' results is shown in Table 2.

It is observed that the proposed method gave much better result than BCOSFIRE filter (Azzopardi et al., 2015), a popular technique in vessel delineation, by around 50% in terms of sensitivity. The overall accuracy of the proposed method is around 5% better than the BCOSFIRE result.

Table 2: Comparison of results of various vessel delineation methods.

	BCOSFIRE	Frangi's Vesselness	Proposed Method
Sensitivity	20.22%	75.24%	71.77 %
Specificity	93.65 %	86.16%	94.57 %
Accuracy	88.68%	85.42%	93.03%

The results were also compared with Frangi's vesselness method on which the proposed method is based. The overall accuracy and specificity of the proposed method was found to be better by 8%. This is the result of the proposed method's focus on removing falsely identified edges as blood vessel edges. The sensitivity of Frangi's method was better by around 3.5%. This is because the proposed method while removing false edges sometimes also removed a few true edges. This is acceptable as our final aim is to obtain accurate blood vessel information. So, our effort is oriented towards minimizing information from false blood vessel edges, and in this process it is tolerable to lose some true blood vessels as this blood vessel information can also be obtained from other identified blood vessels. Illustrative images with results improved by the proposed method are shown in Fig. 12.

4 CONCLUSION AND FUTURE WORK

The paper proposed a novel method for scene classification for endoscopic images into classes, based on ink and blood vessel content using SVM with Cubic kernel. The features were based on colour, edges information and texture. The blood vessel containing non-dyed images were used for blood vessel extraction. The blood vessel extraction process is based on the Frangi vesselness filter. The originality added by the proposed method lies in its ability to differentiate the edges extracted by Frangi filter into blood vessel and non-blood vessel edges. The proposed algorithm achieves this aim by doing background subtraction and filtering using a custom intensity-based dissymmetry detection filter. Blood vessel delineation for dyed images is a topic of future work. Another work is to apply this research to 3D recovery of polyp with absolute size and shape for supporting medical image diagnosis.

ACKNOWLEDGEMENT

This research was done while Mayank Golhar visited Iwahori Lab. of Chubu University for his research internship. Iwahori's research is supported by JSPS Grant-in-Aid for Scientific Research (C) (#26330210) and (B) (#15H02768), and Chubu University Grant.

REFERENCES

Azzopardi, G., Strisciuglio, N., Vento, M., and Petkov, N. (2015). Trainable cosfire filters for vessel delineation with application to retinal images. *Medical image analysis*, 19(1):46–57.

Frangi, A. F., Niessen, W. J., Vincken, K. L., and Viergever, M. A. (1998). Multiscale vessel enhancement filtering. In *International Conference on Medical Image Computing and Computer-Assisted Intervention*, pages 130–137. Springer.

Fraz, M. M., Remagnino, P., Hoppe, A., Uyyanonvara, B., Rudnicka, A. R., Owen, C. G., and Barman, S. A. (2012). Blood vessel segmentation methodologies in retinal images–a survey. In *Computer methods and programs in biomedicine, Vol. 108(1), pp. 407-433*. Elsevier.

Hafner, M., Gangl, A., Wrba, F., Thonhauser, K., Schmidt, H.-P., Kastinger, C., Uhl, A., and Vecsei, A. (2007). Comparison of k-nn, svm, and nn in pit pattern classification of zoom-endoscopic colon images using cooccurrence histograms. In *Image and Signal Processing and Analysis, 2007. ISPA 2007. 5th International Symposium on, pp. 516-521*. IEEE.

Ikeda, N., Usami, H., Iwahori, Y., Bhuyan, M., and Kasugai, K. (2016). Generating lambertian image by removing specular reflection component and difference of reflectance factor using hsv. In *Proc. of ITC-CSCC 2016, T2-5, Computer Vision (2), pp.547-550*.

Kumar, V., Abbas, A. K., Fausto, N., and Aster, J. C. (2014). *Robbins and Cotran pathologic basis of disease*. Elsevier Health Sciences, 9th edition.

Lin, B., Sun, Y., Sanchez, J. E., and Qian, X. (2015). Efficient vessel feature detection for endoscopic image analysis. *IEEE Transactions on Biomedical Engineering*, 62(4):1141–1150.

Mohanty, A. A., Vaibhav, B., and Sethi, A. (2013). A frame-based decision pooling method for video classification. In *2013 Annual IEEE India Conference (INDICON)*, pages 1–5. IEEE.

Zhang, D., Wong, A., Indrawan, M., and Lu, G. (2000). Content-based image retrieval using gabor texture features. In *IEEE Pacific-Rim Conference on Multimedia, University of Sydney, Australia*, pages 392–395.